JOURNAL OF BACTERIOLOGY, Dec. 1996, p. 7159–7166 Vol. 178, No. 24
0021-9193/96/$04.00+0


# Use of Green Fluorescent Protein To Visualize the Early Events of Symbiosis between *Rhizobium meliloti* and Alfalfa (*Medicago sativa*)

DANIEL J. GAGE, TANYA BOBO,† AND SHARON R. LONG*

*Department of Biological Sciences, Stanford University, Stanford, California 94305-5020*

Received 6 May 1996/Accepted 30 August 1996

**A gene encoding a variant of green fluorescent protein (GFP) of *Aequorea victoria* was put under the control of a promoter which is constitutive in *Rhizobium meliloti*. The heterologous GFP gene was expressed at high levels during all stages of symbiosis, allowing *R. meliloti* cells to be visualized as they grew in the rhizosphere, on the root surface, and inside infection threads. In addition, nodules that were infected with bacteria which were synthesizing GFP fluoresced when illuminated with blue light. GFP-tagged bacteria could be seen inside infection threads, providing the opportunity to measure the growth rate and determine the patterns of growth of *R. meliloti* residing inside its host plant.**

Bacteria belonging to the genera *Rhizobium*, *Bradyrhizobium*, and *Azorhizobium* grow as free-living organisms in the soil and can also live as nitrogen-fixing symbionts inside root nodule cells of plants belonging to the family Leguminosae. The symbiosis between *Rhizobium meliloti* and its host alfalfa begins when bacteria growing in the soil are attracted toward and bind to host root hairs. There, the bacteria respond to compounds secreted by the plant root by transcribing *nod* genes, which direct the synthesis of a lipooligosaccharide signal molecule, the Nod factor, which initiates many of the developmental changes seen in the root early in the nodulation process (7, 12, 29). These changes include root hair deformation, membrane depolarization, and the initiation of cell division in the inner root cortex, which establishes a nodule primordium (10, 12, 24). The infection thread, which is a tubule containing dividing and growing bacteria, extends down through the root hair and then traverses several cell layers to deliver bacteria to root cells in the developing nodule. Bacteria exit the infection thread, and these bacteria differentiate and fix atmospheric nitrogen, which is exported from the nodule to the rest of the plant.

Infection thread formation begins when bacteria, growing in the rhizosphere or on the root surface, become trapped between two epidermal root hair cell walls. This occurs most often when a deformed root hair forms a sharp bend or curl in such a way that bacteria bound to the cell become trapped between appressed cell walls (4, 11, 31). Less frequently, infection threads originate at the junction of a root hair branch or at the point where two root hairs press against one another (4, 11, 31). Data from ultrastructural studies indicate that initiation of infection thread growth involves an alteration of the root hair cell wall, followed by invagination of the cell wall and extension of the incipient tubule by tip growth (4, 15, 23). The infection thread grows along the root hair axis and into the body of the epidermal cell. If the infection thread exits this cell, it does so by fusing with the distal cell wall, and bacteria enter the intercellular space. A process of invagination and tip growth, similar to that seen at the beginning of infection thread growth, occurs in the adjacent cell, and the thread is propagated further toward the inner root cortex (25–27). Bacterial cells inside the infection thread eventually enter nodule cells through a process which appears to involve binding of the bacteria to the root cell cytoplasmic membrane and uptake into the cells by endocytosis. Branching of the thread as it enters the nodule primordium leads to an increase in the number of sites from which bacteria can exit the thread and enter nodule cells, ensuring that a sufficient number of cells are occupied during the nodulation process. Once inside the root cells, the bacteria differentiate and begin to synthesize proteins required for nitrogen fixation and the maintenance of the mutualistic partnership.

Many interesting questions concerning the growth and behavior of the bacteria during the early stages of infection remain unanswered owing to the difficulty of monitoring the growth of the bacteria on the surface of the root, on the tips of the root hairs, and inside the infection thread. For example, it is not known where bacterial cell division takes place in the infection thread and whether cells divide throughout this structure or only at certain locations in the thread such as at the growing tip. It is also not known if bacterial growth is coupled to thread elongation in the sense that bacteria increase in number only if the plant-derived part of the thread is elongating.

Chalfie et al. have recently described the use of green fluorescent protein (GFP) as a marker for studying cell-specific gene expression in living tissue (5). GFP is a small protein found in the jellyfish *Aequorea victoria*. It has the property of fluorescing when excited by UV or short-wave blue light (5, 14). The chromophore is made of three contiguous amino acids near the amino terminus of the protein, and it requires no exogenous cofactors for fluorescence (5, 6). This means that when the gene for GFP is put under the control of a heterologous promoter, the timing and spatial expression of the promoter can be studied in real time, in living tissue; no fixing or staining of the organism is required to monitor GFP expression. This paper describes the construction of plasmids which allow for the constitutive expression of wild-type and variant GFPs and their use for visualizing the growth and behavior of *R. meliloti* during the early stages of infection and nodulation.

## MATERIALS AND METHODS

**Bacterial strains.** *R. meliloti* Rm1021 is a streptomycin-resistant derivative of the wild-type strain SU47 (20). *R. meliloti* MB501 is a derivative of strain Rm1021

* Corresponding author. Phone: (415) 723-3122. Fax: (415) 725-8309.
† Present address: Cornell University, Ithaca, N.Y.

TABLE 1. Strains and plasmids used in this study

| Strain or plasmid | Relevant characteristics | Source or reference |
|---|---|---|
| *R. meliloti* | | |
| Rm1021 | Sm$^r$ | 20 |
| MB501 | Derivative of Rm1021 which can be transformed by electroporation; Sm$^r$ Tm$^r$ | This lab |
| Plasmids | | |
| pBlueScript SK(+) | Ap$^r$ | Stratagene |
| pVO131 | 152-bp *Pvu*I-*Hpa*II fragment of *S. typhimurium trp* promoter linked into the *Hin*dIII site of pBlueScript SK(+); Ap$^r$ | This lab |
| pBBR1MCS | Cm$^r$ | 17 |
| pMB393 | Spectinomycin-resistant derivative of pBBR1MCS; Sp$^r$ Cm$^r$ | This lab |
| pGFP101.1 | GFP cloned into pBlueScript SK(+) | 5 |
| pTB1G | GFP cloned downstream of p*trp* in pVO131; Ap$^r$ | This lab |
| pTB1F | GFP-S65T[a] cloned downstream of p*trp* in pVO131; Ap$^r$ | This lab |
| pTB93G | p*trp*-GFP in pMB393. Sp$^r$ Cm$^r$ | This lab |
| pTB93F | p*trp*-GFP-S65T[a] in pMB393. Sp$^r$ Cm$^r$ | This lab |

[a] GFP-S65T mutant of GFP which contains threonine rather than serine at amino acid residue 65.

which contains a Tn*5* carrying trimethoprim resistance. This insertion greatly increases the frequency with which the bacteria can be transformed by electroporation (1). The bacteria and plasmids used in this study are listed in Table 1.

**GFP expression plasmids.** The GFP gene was amplified by using pGFP10.1 as a template (5). The sequence of the 5′ and 3′ primers used for amplification (primers 1 and 3 in Fig. 1A) were such that an *Eco*RI site and a prokaryotic ribosome-binding site were inserted upstream of the GFP open reading frame and a *Sma*I site was introduced downstream of the same open reading frame (Fig. 1A). This altered GFP gene was then cloned downstream of the *Salmonella typhimurium trp* promoter in pVO131 (22), resulting in plasmid pTB1G (Fig. 1B). A version of pTB1G which contained threonine at amino acid residue 65 of GFP instead of serine was also made. This was done by amplifying a piece of DNA from plasmid pGFP10.1 with primer 2 and primer 3 (Fig. 1A) and exchanging the *Msc*I-*Bst*BI fragment in pTB1G, which contains the fluorescent center, with the *Msc*I-*Bst*BI fragment generated from the amplification product. The resulting plasmid was named pTB1F. The ptrp-GFP transcriptional fusions were removed from plasmids pTB1G and pTB1F as *Pst*I-*Kpn*I fragments and cloned into pMB393. The resulting plasmids were named pTB93G and pTB93F, respectively. Plasmid pMB393 was made by cloning a 2.4-kb *Bam*HI-*Eco*RI fragment of Tn*21*, which contains a spectinomycin resistance gene, into the *Ear*I site of pBBR1MCS, a broad-host-range vector, derived from a *Bordetella bronchiseptica* plasmid (1, 17).

**Plant growth and inoculation.** Alfalfa (*Medicago sativa* cv. AS13) seeds were surface sterilized by shaking for 45 min in 95% ethanol and then for 15 min in a solution of 5.25% sodium hypochlorite. The seeds were washed extensively with sterile water and allowed to germinate for 3 days in the dark. Three seedlings, 1 to 2 cm long, were placed on a sterile microscope slide which had been overlaid with 2 ml of BNM medium (10) in 0.8% agarose. The plants were inoculated with 0.1 ml of bacterial suspension. The inoculated plants were covered with a single layer of washed dialysis membrane (12-kDa molecular size cutoff). The slide was then placed in a 50-ml conical culture tube containing 5 ml of BNM, and the tube was placed a growth chamber (26°C, 16-h/8-h light/dark period).

Bacterial suspensions were made by resuspending colonies picked from an LB plate to an optical density at 595 nm of about 0.1 in sterile water. The cells were washed once with sterile water and diluted 1:100 or 1:1,000 in sterile water. These dilutions were used for inoculating seedlings. We noticed that inoculating plants with larger numbers of bacteria seemed to inhibit infection thread formation.

**Microscopy.** Fluorescence microscopy was done on a Nikon Optiphot inverted microscope stand, and images were captured with a Hamamatsu SIT video camera or on Kodak Ektachrome Elite 400 film. The filter set for fluorescence microscopy consisted of a 470- to 490-nm band-pass excitation filter and a 520- to 560-nm barrier filter. Propidium iodide staining was done by soaking tissue in a 10-μg/ml solution of propidium iodide in BNM medium for at least 30 min. The tissue was destained in BNM medium for at least 30 min. Confocal microscopy was done on either a Molecular Dynamics MultiProbe 2010 or a Leica TCS 4D microscope. GFP-S65T was excited with the 488-nm laser line, and the barrier filter had a 520-nm cutoff. Propidium iodide-stained tissue was excited with the 568-nm laser line, and the barrier filter had a 590-nm long-pass cutoff. Confocal images were reconstructed with NIH Image software, and images were colorized and prepared for publication with Adobe Photoshop software.

Propidium iodide staining was performed on fresh tissue, which was excised from plants immediately before staining and microscopy. All other microscopy was performed on live, intact plants.

## RESULTS

**Construction of plasmids which constitutively express GFP.** To monitor *R. meliloti* during the early stages of the process which leads to nodulation, we constructed bacterial strains that constitutively expressed GFP or a variant of this protein which differed from the wild type by having a threonine instead of serine at amino acid residue 65. This variant, GFP-S65T, has features which make it superior to GFP for studying nodulation in plants. First, its main excitation peak is at 489 nm, rather than at 396 nm (14). GFP does absorb at 489 nm, but the intensity of emitted light is rather weak. Illumination of GFP-S65T at 489 nm was preferable to illumination of GFP at 396 nm for several reasons: it is less damaging to bacterial cells and plant tissue; the chromophore photobleaches less quickly; and the autofluorescence of the plant cell wall is much reduced. In addition, it has been shown that the GFP-S65T variant matures from the nonfluorescent form to the fluorescent form much more quickly than does GFP (13). This maturation results from an oxidation and the cyclization of the three amino acids which make up the chromophore (14). We found that *R. meliloti* cells expressing the GFP-S65T variant were much brighter when inside nodules than were bacteria expressing GFP (Fig. 2A and B and data not shown). This may be because the GFP-S65T variant is more likely to form an active chromophore under the low oxygen tensions which prevail in the nodule than is GFP.

We cloned GFP and GFP-S65T, altered the region immediately 5′ of the start of the open reading frame such that each gene would have a good bacterial ribosome-binding site, and then placed each gene under the control of a fragment of the *Salmonella typhimurium trp* promoter. This *trp* promoter fragment is constitutively active in *R. meliloti* and results in high levels of expression of genes placed under its control (9). The p*trp*-GFP and p*trp*–GFP-S65T fusions were cloned into a broad-host-range vector derived from a *Bordetella bronchiseptica* plasmid (17). The construction of these plasmids is outlined in Figure 1.

*R. meliloti* containing plasmid pTB93F expressed GFP-S65T and fluoresced brightly without observable aggregation of the protein into inclusion bodies (Fig. 1C).

Because spectinomycin, the antibiotic used to select for maintenance of the broad-host-range GFP expressing plasmids, is toxic to plants, we had to inoculate plants with bacteria in the absence of selection for plasmid maintenance. Microscopic examination showed that the majority of nodules and infection threads were populated with bacteria that expressed GFP. However, there was a fraction of both nodules and infection threads that did not contain bacteria expressing GFP. To assess plasmid stability in the absence of selection, we grew strain MB501/pTB93F for approximately 25 generations in Luria-Bertani (LB) growth medium without antibiotic selection and monitored plasmid loss. The results, presented in Fig. 3, show that about 60% of the bacterial cells retained the plasmid at the end of the experiment. This corresponded to the fre-

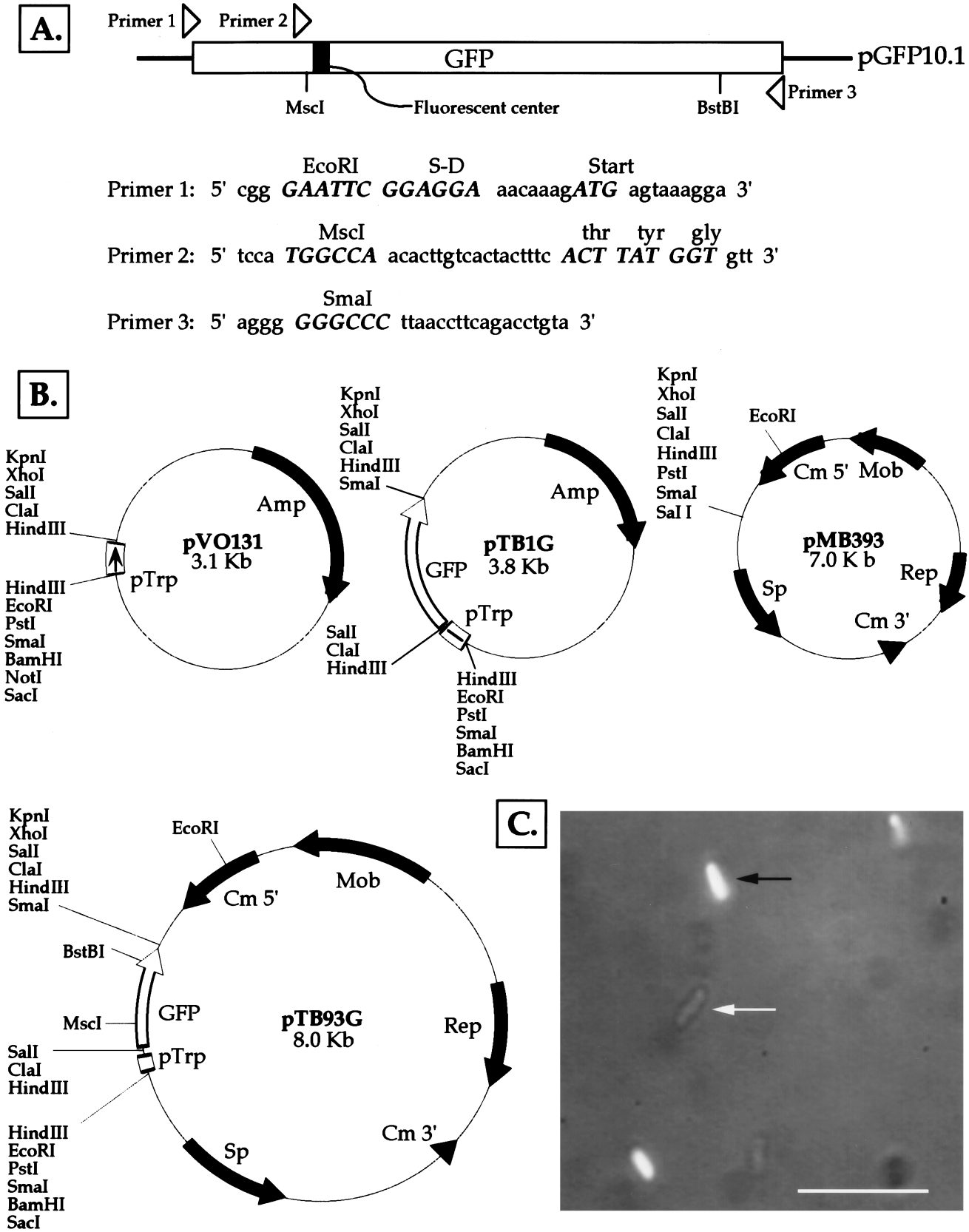


FIG. 1. GFP expression plasmids. (A) Location of the primers used to amplify the GFP gene from the template plasmid pGFP10.1. Also shown is the location of the fluorescent chromophore and the primer used to change amino acid 65 from serine to threonine. (B) Map of plasmid pTB93G and the plasmids used in its construction. Plasmids pTB1F and pTB93F (not shown) are identical to plasmids pTB1G and pTB93G, except that they contain a single base change which results in the GFP-S65T mutation. (C) *R. meliloti* MB501/pTB93F was mixed with *R. meliloti* MB501, which did not contain the plasmid, and viewed by fluorescence microscopy. The dark arrow indicates a fluorescent bacterium expressing GFP-S65T, and the light arrow indicates a nonfluorescent bacterium, presumably strain MB501 without pTB93F. Bar, 3 μm.

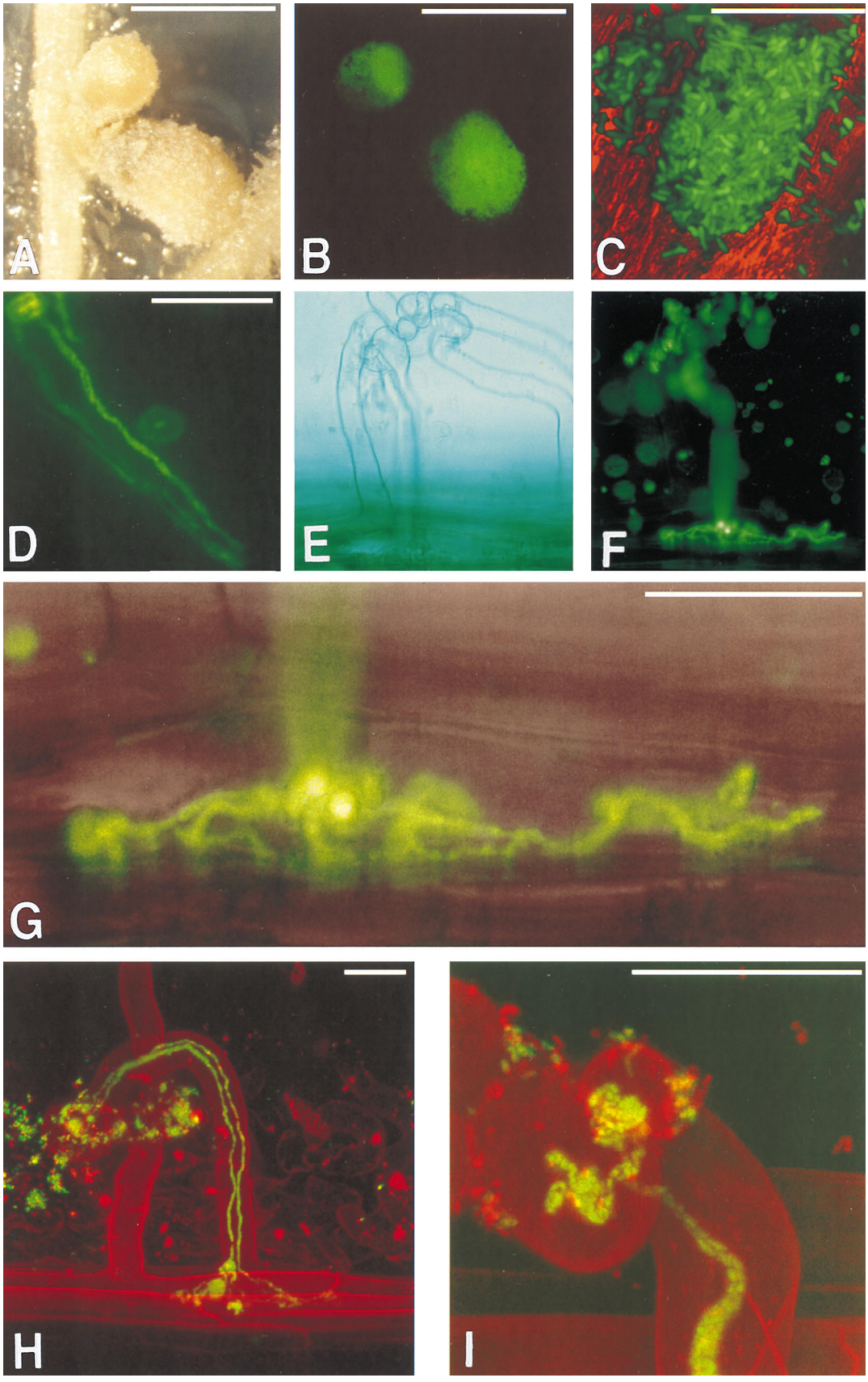
A
B
C
D
E
F
G
H
I

FIG. 2. Visualization of infection events by using *R. meliloti* expressing GFP-S65T. (A) Bright-field image of two alfalfa nodules induced by strain MB501/pTB93F. (B) Same nodules as shown in panel A viewed under fluorescent microscopy. (C) Confocal reconstruction of a microcolony of strain MB501/pTB93F growing on the surface of an alfalfa root. The surface of the epidermal cells (red) was imaged with reflected laser light; bacteria were imaged by fluorescence. The colony is growing at the junction of two epidermal cells whose long axes run diagonally from the lower left to the upper right. (D) Video image of strain MB501/pTB93F growing inside infection threads. The three threads initiated out of frame to the upper left and are growing toward the lower right. Individual bacteria can be seen inside the threads. (E) Bright-field image of a root hair cell body containing an infection thread. The infection thread can be seen branching as it enters the cell body. (F) Fluorescence microscopy image of the same cells shown in panel E. (G) Combined fluorescence and bright-field images of the infection thread in panels E and F. The infection thread in the root hair is out of focus and gives rise to the vertical smudge of fluorescence seen on the left side of the micrograph. (H) Confocal reconstruction of a root hair with a double infection thread. Green represents GFP fluorescence, and red represents the fluorescence of the propidium iodide counterstain. The threads start in the curled portion of the root hair at the left of the micrograph, proceed down the hair, and branch when they enter the cell body. Fluorescent bacteria can be seen embedded in the root mucigel to the left of the infected root hair. (I) Confocal reconstruction of an infection thread. Coloring is the same as in panel H. Columns of individual bacteria can be seen inside the thread, and individual fluorescent bacteria can also be seen bound to the surface of the root hair. Panels B to D and G to I have been colorized by computer. An attempt was made to faithfully reproduce the luminosity and color of the GFP-S65T fluorescence as it was seen through the fluorescence microscope. Panels E and F have not been artificially colored and therefore reflect the color and luminosity of the structures as seen through the microscope. Bars, 3 mm for panels A and B, 20 μm for the other panels.

quency of nodules and infection threads inhabited by GFP-expressing bacteria seen during microscopic examination of infected plants.

**Visualization of early infection events using *R. meliloti* expressing GFP-S65T.** Alfalfa seedlings used in this study were inoculated with about $10^5$ cells of strain MB501/pTB93F. At 1 day after inoculation, few bacteria were seen on or near the plant root. By day 3, many bacteria were associated with the root system, and their numbers increased for up to 2 weeks. Bacteria could be seen growing embedded in the mucigel surrounding the root (Fig. 2H), on root hairs (Fig. 2I), and in microcolonies growing on the root surface, often at the junction of two epidermal cells (Fig. 2C). In most cases, the root tissue appeared healthy even when heavily colonized by bacteria.

Infection threads could be easily seen, and their overall structure corresponded to that observed in ultrastructural studies (2, 15) and in studies with fixed and stained tissue (4, 11, 16, 28). The threads most often started from microcolonies of bacteria trapped in curled root hair tips (Fig. 2H). The threads contained a column of bacteria which progressed down the root hair and often branched once or twice before it entered the body of the epidermal cell (Fig. 2D and H). In many cases, the thread branched many times as soon as it left the root hair and entered the epidermal cell body (Fig. 2E to H; also see Fig. 4G). Infection threads which were seen in the first week after inoculation had bacterial columns which were usually two to four bacteria wide. The bacteria were generally oriented with their long axis parallel to the long axis of the infection thread (Fig. 2D, H, and I; also see Fig. 4G).

**Dynamics of infection thread growth.** One of the most useful aspects of GFP for biological studies is that it can be monitored in living tissue, in real time, with minimal disruption of the system under investigation. These characteristics make GFP ideal for studying the behavior of *R. meliloti* growing inside infection threads. Figure 4A shows an infection thread inside a root hair, and Fig. 4B shows the same infection thread 6 h later. The length of the thread has increased by about 50% over this period, corresponding to a rate of lengthening of 15 μm/h. This is comparable to the rate of 5 to 8 μm/h estimated by Fahraeus for infection thread growth in clover (11). Assuming that the bacteria are growing exponentially throughout the whole structure, and assuming that all bacterial growth results in an increase in thread length and not in thread diameter, then the growth of the thread over the 6 h would indicate a bacterial doubling time of about 11 h. *R. meliloti* grown in batch culture in a rich medium has a doubling time of about 4 h, and its doubling time in a glucose minimal medium is not much longer. The apparent difference between the growth rate in batch culture and the growth rate inside the infection thread may reflect slower, or nonexponential, growth inside the plant. Alternatively, the apparent slow growth may arise because not all bacteria throughout the thread are growing, or because some of the bacterial growth contributes to a widening of the thread rather than a lengthening of it.

Figure 4C shows an infection thread that had progressed down a root hair and just entered the body of the epidermal cell. The thread was a mosaic: it had sectors where the bacteria no longer expressed GFP-S65T. This was probably due to loss of pTB93F as bacteria grew on the plant surface and to subsequent infection of the root hair by a mixed population of bacteria, some of which no longer synthesized GFP. In support of this idea, we have been able to generate such mosaic patterns simply by inoculating plants with a mixture of fluorescent and nonfluorescent *R. meliloti* strains. If bacterial cells maintained their position with respect to each other as the colony inside the thread grew and moved down the root hair, then the

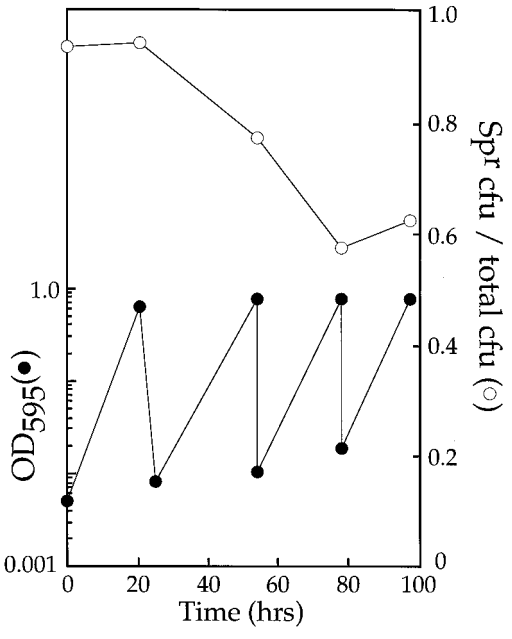


FIG. 3. Maintenance of plasmid pTB93F in the absence of selection. Typical results from an experiment done to determine plasmid stability are shown. *R. meliloti* MB501/pTB93F was grown overnight in LB medium with spectinomycin and diluted the next day into LB medium without spectinomycin. The culture was allowed to grow to saturation and then diluted. This was done four consecutive times over the course of the experiment. The proportion of spectinomycin-resistant bacterial cells was determined by plating at the indicated times. The upswing in the number of spectinomycin-resistant cells at the end of the experiment is probably insignificant and may be due to sampling error. $OD_{595}$, optical density at 595 nm.

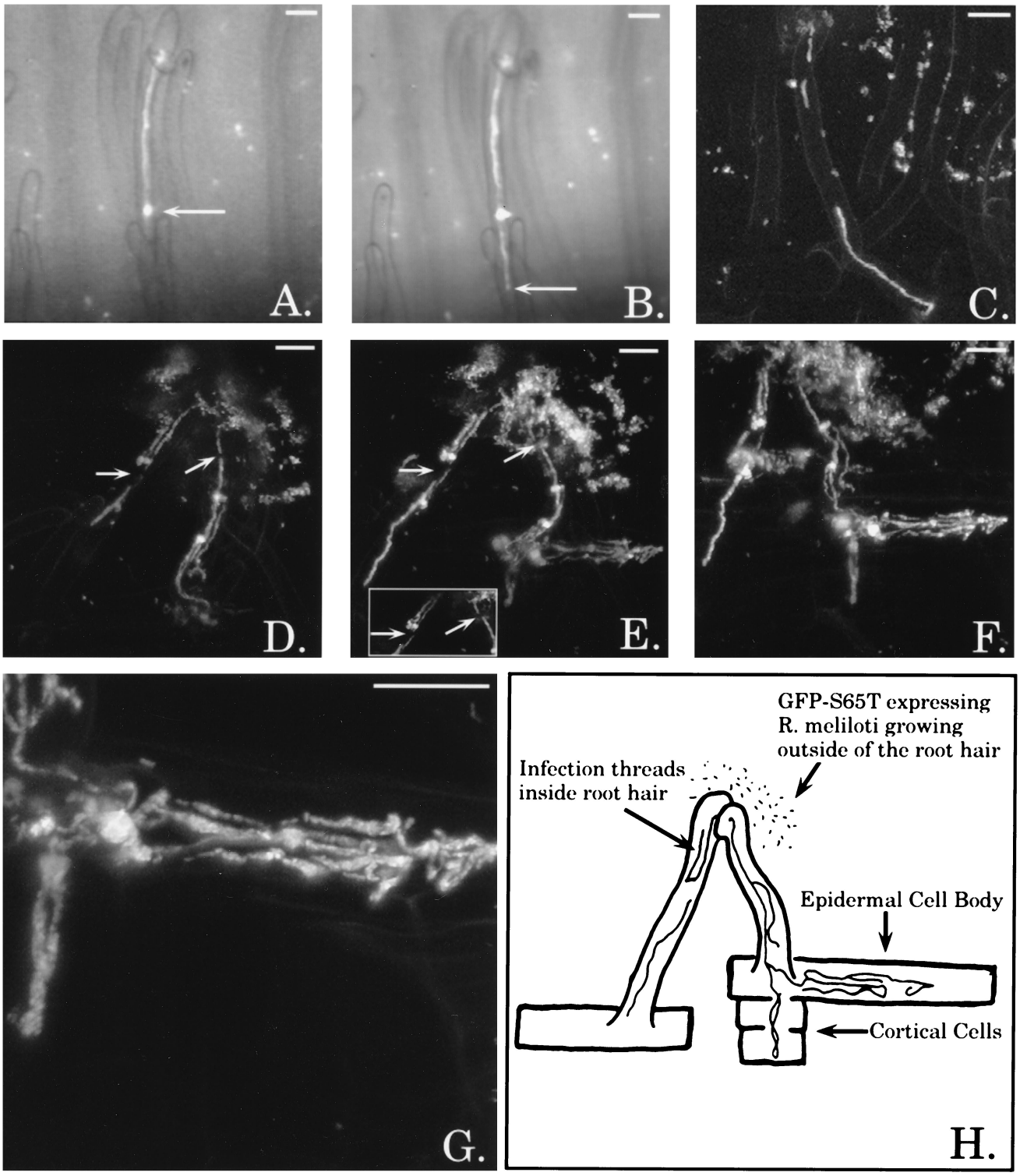


FIG. 4. Growth of bacteria inside infection threads. (A) An infection thread populated with *R. meliloti* MB501/pTB93F. The tip of the thread is indicated by the arrow. (B) The infection thread in panel A after 6 h of growth. The thread has lengthened, and the location of the tip is indicated by the arrow. (C) Confocal reconstruction of a root hair containing a sectored infection thread. (D) Confocal reconstruction of two root hairs containing infection threads. Arrows indicate dark sectors in the threads. (E) Confocal reconstruction of the infection threads shown in panel D after 24 h of growth. Arrows indicate the same dark sectors indicated in the previous panel. The inset contains a reconstruction of the threads by using only some of the optical sections used to generate the larger image. By discarding sections which contain images of the bacteria growing on top of the root hair, the rightmost dark sector can be more easily seen. (F) Confocal reconstruction of the infection threads shown in panel D after 48 h of growth. (G) Confocal reconstruction of ramified infection threads inside the epidermal cell body of the rightmost infected cell in panel F. (H) Schematic diagram showing the locations of structures present in panels D to F. Bars, 20 μm.

sectoring pattern should reflect the pattern of fluorescent and nonfluorescent bacteria present shortly after the initiation of infection thread formation. Alternatively, the GFP expression plasmid may have been lost from cells as they grew inside the infection thread and thereby given rise to the dark sectors. Such sectors should be small unless they were generated early during the course of thread growth: a single bacterium which lost the ability to express GFP would form a large, dark sector only after many cell doublings. The dark and light sectors present in the bottom half of the infection thread shown in Fig. 4C are relatively large and may be the result of clonal expansion of sectors which were present early during infection. The dark sectors at the top of the thread are smaller than those at the bottom. This may be because they arose later during growth of the thread and have not had much time to expand; alternatively, it may be that the sectors were present early but bacteria in the upper portion of the thread grew for only a limited period.

Figure 4D shows branched infection threads inside two root hairs 3 days after the plant was inoculated with *R. meliloti* which expressed GFP-S65T. The same threads, 24 h later, are shown in Fig. 4E. The rightmost thread entered the epidermal cell body, ramified, and penetrated into an underlying cortical cell. The total increase in the length of the thread was about fourfold, indicating that the bacteria were growing with a doubling time of approximately 12 h. This assumes that all of the bacteria in the thread were growing and contributing to the increase in thread length. The other thread in the figure increased in length by about 50% over the same period. Both threads contained small dark sectors, and interestingly, these sectors, and the bright sectors behind them did not expand or change position, even though the total length of the thread had increased (Fig. 4D and E). This indicates that bacteria which were not near the tip of the thread were static and did not contribute to the growth of the thread. This implies that the growth of the bacteria near the tip, which are actively dividing, is faster than the 11- to 12-h doubling time estimated by simply measuring the change in thread length over a given period.

## DISCUSSION

GFP is a useful tool for monitoring gene expression and protein localization (5, 21, 30), cytoskeletal structure and dynamics (19), bacterium-host interactions in models of mammalian pathogenic interactions (8, 18), and viral infection and virus movement in plant systems (3).

In this paper, we describe the construction of a broad-host-range plasmid that constitutively expresses GFP or the S65T variant of GFP. These plasmids are stable in the absence of selection, and bacterial strains containing them are able to colonize roots and form nodules on alfalfa.

Throughout the time when *R. meliloti* is growing on and inside its host plant, individual bacteria are not easily discerned by conventional light microscopy, and microscopic methods which involve fixation or staining to better resolve the bacteria necessarily destroy the investigator's ability to monitor dynamic interactions between the two partners. The ability to easily visualize individual bacterial cells by using GFP as a marker makes it feasible to address some fundamental questions concerning the growth, distribution, and movement of *R. meliloti* during the nodulation process.

Bacterial growth inside the infection thread is particularly amenable to study by using GFP. The thread is transparent, and individual GFP-expressing bacteria can be observed during the process of growth inside the tubule. The growth of bacteria inside this structure is intriguing, because it is a point at which bacterial growth needs to come under the control of the plant host. Bacterial growth normally remains constrained such that the bacterial cells do not overrun the thread. Infection threads, both in root hairs and also inside the developing nodule, typically contain two to four columns of bacteria across the width of the structure. A mutant strain of *R. meliloti* in which bacterial growth inside the infection thread is no longer normal has been isolated (unpublished results). Plants inoculated with this mutant form infection threads containing many times the usual number of bacteria.

We have shown in this paper that infection threads lengthen at rates which would imply very slow growth of *R. meliloti* if it is assumed that all bacterial cells in the thread are growing. However, observation of fluorescent and nonfluorescent bacterial sectors in developing infection threads indicated that bacteria in older parts of the thread were not growing and therefore were not contributing to the lengthening of the thread. This means that the bacteria near the tip, which were growing, were doing so at rate which was underestimated by measuring the change in total thread length over a given time. Therefore, the actual growth rate of bacteria near the tip of the infection thread was probably faster than the 11 to 12 h per generation inferred from the rate of increase in total thread length. These observations raise the question of how bacteria inside the infection thread can grow at different rates depending on their position along the length of the thread. The possibilities range from an active type of growth control in which bacteria sense their position relative to the growing infection thread tip and regulate their rate of increase accordingly to a more passive type of control in which the plant limits the capacity for bacterial increase by limiting nutrients to cells in distant parts of the thread. As an example of the latter possibility, it may be that nutrients are delivered only to the tip of the thread, resulting in a gradient of nutrients which decreases from the tip to the base of the structure.

One consequence of having only the bacteria in the tip region of the thread divide and move along the thread as it grows is that most of the bacteria which originally entered the infection thread from the outside environment will grow down the infection thread a short distance and then cease growing. This means that if bacteria other than *R. meliloti* entered the thread, they would not progress into the root proper unless they happened to be located at the very tip of the thread. In such a case, the plant may terminate thread growth. Termination of thread growth often occurs during *R. meliloti* infection of alfalfa and is proposed to play a role in determining the number of nodules a plant develops (28). It may also play a role in preventing unwanted species from entering the plant root through infection threads. The use of in vivo markers such as GFP may permit the direct observation of bacterium-host interactions, both of successful invading strains and of unsuccessful strains or species, providing a means of studying how the choice to terminate or allow infection thread growth is made by the plant.

## ACKNOWLEDGMENTS

We thank David Ehrhardt and Rebecca Wais for help with microscopy and for providing some of the confocal images used in this paper. We also thank Valerie Oke and Melanie Barnett for providing us with vectors used in this study.

S.R.L. is an Investigator of the Howard Hughes Medical Institute. This work was also supported by NIH grant GM30962 and by NIH Research Service Award GM16211 to D.J.G. T.B. was supported by the Minority Summer Research Exchange Program at Stanford University.

## REFERENCES


1. **Barnett, M., L. Zumstein, and W. Margolin.** Personal communication.
2. **Bassett, B., R. N. Goodman, and A. Novacky.** 1977. Ultrastructure of soybean nodules. I. Release of rhizobia from the infection thread. Can. J. Microbiol. **23:**573–582.
3. **Baulcombe, D. C., S. Chapman, and S. S. Cruz.** 1995. Jellyfish green fluorescent protein as a reporter for virus infections. Plant J. **7:**1045–1053.
4. **Callaham, D. A., and J. G. Torrey.** 1981. The structural basis for infection of root hairs of *Trifolium repens* by *Rhizobium*. Can. J. Bot. **59:**1647–1664.
5. **Chalfie, M., Y. Tu, G. Euskirchen, W. W. Ward, and D. C. Prasher.** 1994. Green fluorescent protein as a marker for gene expression. Science **263:**802–805.
6. **Cody, C. W., D. C. Prasher, W. M. Westler, F. G. Prendergast, and W. W. Ward.** 1993. Chemical structure of the hexapeptide chromophore of the *Aequorea* green fluorescent protein. Biochemistry **32:**1212–1218.
7. **Denarie, J., F. Debelle, and C. Rosenberg.** 1992. Signaling and host range in nodulation. Annu. Rev. Microbiol. **46:**497–525.
8. **Dhandayuthapani, S., L. E. Via, C. A. Thomas, P. M. Horowitz, D. Deretic, and V. Deretic.** 1995. Green fluorescent protein as a marker for gene expression and cell biology of mycobacterial interactions with macrophages. Mol. Microbiol. **17:**901–912.
9. **Egelhoff, T. T., and S. R. Long.** 1985. *Rhizobium meliloti* nodulation genes: identification of *nodDABC* gene products, purification of *nodA* protein, and expression of *nodA* in *Rhizobium meliloti*. J. Bacteriol. **164:**591–599.
10. **Ehrhardt, D. W., E. M. Atkinson, and S. R. Long.** 1992. Depolarization of alfalfa root hair membrane potential by *Rhizobium meliloti* Nod factors. Science **256:**998–1000.
11. **Fahraeus, G.** 1957. The infection of clover root hairs by nodule bacteria studied by a simple glass slide technique. J. Gen. Microbiol. **16:**374–381.
12. **Fisher, R. F., and S. R. Long.** 1992. *Rhizobium*-plant signal exchange. Nature (London) **357:**655–660.
13. **Helm, R., A. B. Cubitt, and R. Y. Tsien.** 1995. Improved green fluorescence. Nature (London) **373:**663–664.
14. **Helm, R., D. C. Prasher, and R. Y. Tsien.** 1994. Wavelength mutations and posttranslational autoxidation of greenfluorescent protein. Proc. Natl. Acad. Sci. USA **91:**12501–12504.
15. **Jordan, D. C., I. Grinyer, and W. H. Coulter.** 1963. Electron microscopy of infection threads and bacteria in young roots nodules of *Medicago sativa*. J. Bacteriol. **86:**125–137.
16. **Kodama, A.** 1989. A comparative light microscopic study of two types of root nodule bacteria dispersal into the bacteroid zone cells. Bot. Mag. Tokyo **102:**381–391.
17. **Kovach, M. E.** 1994. pBBR1MCS: a broad-host-range cloning vector. BioTechniques **16:**800–802.
18. **Kremer, L., A. Baulard, J. Estaquier, O. Poulain-Godefroy, and C. Locht.** 1995. Green fluorescent protein as a new expression marker in mycobacteria. Mol. Microbiol. **17:**913–922.
19. **Maniak, M., R. Rauchenberger, R. Albrecht, J. Murphy, and G. Gerisch.** 1995. Coronin involved in phagocytosis: dynamics of particle-induced relocalization visualized by a green fluorescent protein tag. Cell **83:**915–924.
20. **Meade, H. M., S. R. Long, G. B. Ruvkun, S. E. Brown, and F. M. Ausubel.** 1982. Physical and genetic characterization of symbiotic and auxotrophic mutants of *Rhizobium meliloti* induced by transposon Tn*5* mutagenesis. J. Bacteriol. **149:**114–122.
21. **Ogawa, H., S. Inouye, F. I. Tsuji, K. Yasuda, and K. Umesono.** 1995. Localization, trafficking, and temperature-dependence of the *Aequorea* green fluorescent protein in cultured vertebrate cells. Proc. Natl. Acad. Sci. USA **92:**11899–11903.
22. **Oke, V.** Personal communication.
23. **Rae, A. L., P. Bonfante-Fasolo, and N. J. Brewin.** 1992. Structure and growth of infection threads in the legume symbiosis with *Rhizobium leguminosarum*. Plant J. **2:**385–395.
24. **Truchet, G., P. Roche, P. Lerouge, J. Vasse, S. Camut, F. de Billy, J.-C. Promé, and J. Dénarié.** 1991. Sulphated lipo-oligosaccharide signals of *Rhizobium meliloti* elicit root nodule organogenesis in alfalfa. Nature (London) **351:**670–673.
25. **Turgeon, B. G., and W. D. Bauer.** 1985. Ultrastructure of infection-thread development during the infection of soybean by *Rhizobium japonicum*. Planta **163:**328–349.
26. **van Brussel, A. A. N., R. Bakhuizen, P. C. van Spronsen, H. P. Spaink, T. Tak, B. J. J. Lugtenberg, and J. W. Kijne.** 1992. Induction of pre-infection thread structures in the leguminous host plant by mitogenic lipo-oligosaccharides of *Rhizobium*. Science **257:**70–72.
27. **van Spronsen, P. C., R. Bakhuizen, A. A. N. van Brussel, and J. W. Kijne.** 1994. Cell wall degradation during infection thread formation by the root nodule bacteria *Rhizobium leguminosarum* is a two-step process. Eur. J. Cell Biol. **64:**88–94.
28. **Vasse, J., F. de Billy, and G. Truchet.** 1993. Abortion of infection during the *Rhizobium meliloti*-alfalfa sybiotic interaction is accompanied by a hypersensitive reaction. Plant J. **4:**555–566.
29. **Vijn, I., L. das Neves, A. van Kammen, H. Franssen, and T. Bisseling.** 1993. Nod factors and nodulation in plants. Science **260:**1764–1765.
30. **Webb, C., A. Decatur, A. Teleman, and R. Losick.** 1995. Use of green fluorescent protein for visualization of cell-specific gene expression and subcellular protein localization during sporulation in *Bacillus subtilis*. J. Bacteriol. **177:**5906–5911.
31. **Wood, S. M., and W. Newcomb.** 1988. Nodule morphogenesis: the early infection of alfalfa (*Medicago sativa*) root hairs by *Rhizobium meliloti*. Can. J. Bot. **67:**3108–3122.